SHAKEDOWN ANALYSIS OF 3D FRAMES UNDER MULTIPLE LOAD COMBINATIONS USING MIXED FIBER BEAM ELEMENTS

DOMENICO MAGISANO *, LEONARDO LEONETTI * and GIOVANNI GARCEA.*

* Dipartimento di Ingegneria Informatica, Modellistica, Elettronica e Sistemistica
Università della Calabria 87036 Rende (Cosenza), Italy

Key words: Plasticity, fiber analysis, mixed finite element, shakedown, frames

Abstract. This work presents an efficient shakedown analysis of 3D frames under multiple load combinations. Mixed fiber beam FEs are employed for an accurate discretization. The stress admissible domain is defined at fiber level as a function of the load factor using the maximum and minimum effect due to all loads. An incremental-iterative method is used at structural level. It evaluates a fictitious path made of a sequence of safe states with a load factor converging to the safety limit. Each point is obtained by finding kinematic variables corresponding to self-equilibrated stresses satisfying Melan's condition for the current load factor to be safe. An iterative FE state determination provides stress DOFs corresponding to assigned kinematic DOFs and load factor. Important features of the method are: i) a direct application of the Newton method, ii) a computational cost unaffected by dimension and complexity of the load domain, iii) an accurate safety factor using a small number of fibers and iv) an efficient solution for large buildings.

1 INTRODUCTION

If the stress intensity at a certain point of a structure made of ductile materials reaches the yield point, the structure does not necessarily fail or deform excessively. Instead, a certain amount of stress redistribution can take place and some further load increments could be supported. Thus, the actual load-carrying capacity of a structure is generally higher than the elastic limit, sometimes considerably so, as for 3D frames. This consideration has encouraged engineers to exploit this overstrength for a cost-effective design. However, it is important to keep in mind that, during their operational life, structures are subjected to variable loads, whose law of variability in time is often unknown. Instead, it is usually possible to have a good estimate of the variability range in terms of maximum and minimum load amplitude and combination formulas are often available to account for the probability of simultaneous actions. Within this context, shakedown analysis, based on Melan's and Koiter's theorems, is able to provide a reliable safety factor against plastic collapse, loss in functionality due to excessive deformation (ratcheting) or collapse due to low cycle fatigue (plastic shakedown), and also gives valuable information about the internal stress redistribution due to the plastic adaptation. The strain-driven incremental-iterative

shakedown analysis, initially proposed in [1], is a simple and general method applicable to any structural model and FE formulation. It provides a sequence of non-decreasing safe (according to Melan's theorem) load factors converging to the shakedown limit by reconstructing a pseudo-equilibrium path. Compared to a standard path-following elasto-plastic analysis, it requires just a more involved definition of the closest point projection (CPP) scheme used to evaluate FE self-equilibrated and plastically admissible stresses corresponding to a displacement increment, which has to keep into account the range of load variability. The important feature of such an approach is that the global optimization problem of the lower bound theorem is replaced by an iterative global solution plus small-sized optimization problems (CPP) defined at the integration point, or at FE level for mixed interpolations. One of the main open problems is the difficulty in managing the large number of load conditions and the complex combination rules required for a realistic definition of the load domain, which can lead to a very time-consuming analysis. The plastic admissibility is commonly checked in terms of stress resultants, usually axial force and bending moments, through cross section yield functions with multi-surface and/or nonlinear expressions. This aspect, together with the check of plastic admissibility for multiple sections, makes the CPP at FE level a multi-constraint optimization problem in terms of the stress DOFs in order to preserve the equilibrated stress interpolation [2, 3]. In shakedown analysis, the complexity of the section admissibility condition along with the check at multiple sections for all the vertexes of the load domain leads to a huge number of constraints for the CPP problem and to a significantly high computational time for its solution also when external high-performance optimization solvers are employed. The use of a Selection Rule Algorithm [4] only partially simplifies the problem by reducing the number of vertexes of the stress envelope.

This work presents an efficient shakedown analysis of 3D frames under multiple load combinations. Mixed fiber beam FEs are employed for an accurate discretization. The stress admissible domain is defined at fiber level as a function of the load factor using the maximum and minimum effect due to all loads. An incremental-iterative method is used at structural level. It evaluates a fictitious equilibrium path made of a sequence of safe states with a converging non-decreasing load factor. Each point is obtained by finding kinematic variables corresponding to self-equilibrated stresses satisfying Melan's condition for the current load factor to be safe. An iterative FE state determination provides stress DOFs corresponding to assigned kinematic DOFs and load factor. Important features of the method are: i) a direct application of the Newton method, ii) a computational cost unaffected by dimension and complexity of the load domain, iii) an accurate safety factor using a small number of fibers and iv) an efficient solution for large buildings [5].

2   SHAKEDOWN PROBLEM STATEMENT FOR A FIBER MODEL

2.1   3D beam model

Let us consider a cylinder in a reference configuration $\mathcal{B}$, characterized by length ℓ and confined by a lateral boundary, $\partial \mathcal{B}$, and two terminal bases, Ω_0 and Ω_ℓ. The cylinder is referred to a Cartesian frame $(\mathcal{O}, x_1 \equiv s, x_2, x_3)$ with unit vectors $\{\mathbf{i}_1, \mathbf{i}_2, \mathbf{i}_3\}$ and $\mathbf{i}_1$ aligned

with the cylinder axis. In this system (see Fig.1), we denote with $\mathbf{X} = s\mathbf{i}_1 + \mathbf{x}$ the position of a point P, where s is an abscissa which identifies the generic cross-section $\Omega(s)$ of the beam, while $\mathbf{x} = x_2\mathbf{i}_2 + x_3\mathbf{i}_3$ is the position of P inside $\Omega(s)$.
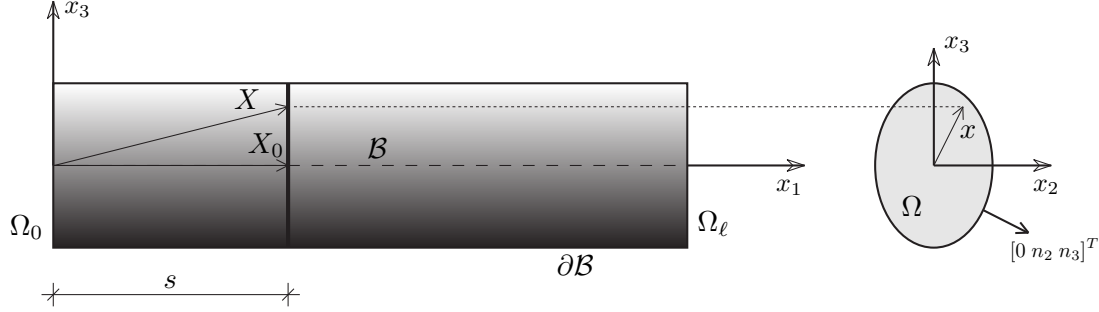

Figure 1: The cylindrical solid.

The displacement field $\mathbf{v}[\mathbf{X}]$ of the model is expressed, as usual, as a rigid motion of the section

$$\mathbf{v}(\mathbf{X}) = \mathbf{u}(s) + \boldsymbol{\varphi}(s) \wedge \mathbf{x} \tag{1}$$

where $\mathbf{u}(s)$ and $\boldsymbol{\varphi}(s)$ are the mean translation and rotation of the section and the operator $\wedge$ denotes the cross product. The kinematics assumed in Eq.(1) allows us to evaluate, using a linear Cauchy continuum, the stress-strain work $\mathcal{W}$ in terms of the generalized strains and stresses on the section as

$$\mathcal{W} := \int_\ell \left(\mathbf{n}(s)^T \boldsymbol{\varepsilon}(s) + \boldsymbol{\tau}(s)^T \boldsymbol{\gamma}(s) \right) ds \tag{2}$$

in which the generalized strains $\boldsymbol{\varepsilon}$, collecting axial strain and bending curvatures, and $\boldsymbol{\gamma}$, collecting shear strains and torsional curvature, are defined as

$$\boldsymbol{\varepsilon}(s) \equiv \begin{bmatrix} e \\ \chi_2 \\ \chi_3 \end{bmatrix} = \begin{bmatrix} u_{1,s} \\ \varphi_{2,s} \\ \varphi_{3,s} \end{bmatrix} \quad \boldsymbol{\gamma}(s) \equiv \begin{bmatrix} \gamma_2 \\ \gamma_3 \\ \chi_1 \end{bmatrix} = \begin{bmatrix} u_{2,s} - \varphi_3 \\ u_{3,s} + \varphi_2 \\ \varphi_{1,s} \end{bmatrix} \tag{3}$$

where a comma stands for derivative. The stress resultants on the section $\mathbf{n}$ and $\boldsymbol{\tau}$ due to normal and tangential stresses respectively are defined as

$$\mathbf{n}(s) = \begin{bmatrix} N_1(s) \\ M_2(s) \\ M_3(s) \end{bmatrix} = \int_\Omega \sigma_{11}(s, \mathbf{x}) \mathbf{a}(\mathbf{x}) d\Omega, \qquad \boldsymbol{\tau}(s) = \begin{bmatrix} N_2(s) \\ N_3(s) \\ M_1(s) \end{bmatrix} = \int_\Omega \begin{bmatrix} \sigma_{12} \\ \sigma_{13} \\ \sigma_{13} x_2 - \sigma_{12} x_3 \end{bmatrix} d\Omega \tag{4}$$

with $\mathbf{a} = [1, x_3, -x_2]^T$. In particular, $\mathbf{n}$ collects axial force and bending moments while $\boldsymbol{\tau}$ collects shear forces and torque. Introducing the vectors

$$\mathbf{t}(s) = \begin{bmatrix} \mathbf{n}(s) \\ \boldsymbol{\tau}(s) \end{bmatrix} \qquad \boldsymbol{\rho}(s) = \begin{bmatrix} \boldsymbol{\varepsilon}(s) \\ \boldsymbol{\gamma}(s) \end{bmatrix} \tag{5}$$

3

we assume an elastic constitutive law expressed as

$$\boldsymbol{\rho}(s) = \mathbf{F}(s)\mathbf{t}(s) \quad \text{with} \quad \mathbf{F}(s)^{-1} = \mathbf{C}(s) = \begin{bmatrix} \mathbf{E} & \mathbf{0} \\ \mathbf{0} & \mathbf{G} \end{bmatrix}. \tag{6}$$

We introduce also the extraction operator $\mathbf{T}_n$ and $\mathbf{T}_\tau$ such that

$$\begin{aligned} \mathbf{n}(s) &= \mathbf{T}_n\mathbf{t}(s), \quad \boldsymbol{\tau}(s) = \mathbf{T}_\tau\mathbf{t}(s), \quad \mathbf{t}(s) = \mathbf{T}_n^T\mathbf{n}(s) + \mathbf{T}_\tau^T\boldsymbol{\tau}(s) \\ \boldsymbol{\varepsilon}(s) &= \mathbf{T}_n\boldsymbol{\rho}(s), \quad \boldsymbol{\gamma}(s) = \mathbf{T}_\tau\boldsymbol{\rho}(s), \quad \boldsymbol{\rho}(s) = \mathbf{T}_n^T\boldsymbol{\varepsilon}(s) + \mathbf{T}_\tau^T\boldsymbol{\gamma}(s). \end{aligned} \tag{7}$$

Finally, using the kinematics in Eq.(1), the normal strain over the section, work-conjugated to $\sigma \equiv \sigma_{11}$, is

$$\epsilon(s, \mathbf{x}) \equiv v_{1,s} = \mathbf{a}(\mathbf{x})^T \boldsymbol{\varepsilon}(s, \mathbf{x}). \tag{8}$$

2.2 Mixed finite element model

The beam finite element adopted (see [4]) uses a stress interpolation

$$\mathbf{t}(s) = \mathbf{L}(s)\boldsymbol{\beta}_e \tag{9}$$

which exactly satisfies the equilibrium equations on the element for zero body forces, that is

$$\boldsymbol{\mathcal{N}},_s = \mathbf{0}, \qquad \boldsymbol{\mathcal{M}},_s + \mathbf{i}_1 \wedge \boldsymbol{\mathcal{N}} = \mathbf{0}, \tag{10}$$

while body load effects are then exactly included as a particular solution. Eq.(10) states that $\boldsymbol{\mathcal{N}} \equiv [N_1, N_2, N_3]^T$ and the torsional moment component M_1 are constant, while the two flexural components $M_2(s)$ and $M_3(s)$ of $\boldsymbol{\mathcal{M}}(s) \equiv [M_1, M_2, M_3]^T$ are linear with s and linked to the shear resultants so that $N_2\ell = -(M_3(\ell) - M_3(0))$ and $N_3\ell = (M_2(\ell) - M_2(0))$. The internal work in Eq.(2) becomes

$$\mathcal{W} \equiv \boldsymbol{\mathcal{N}}^T\left(\mathbf{u}(\ell) - \mathbf{u}(0)\right) + \boldsymbol{\mathcal{M}}(\ell)^T\boldsymbol{\varphi}(\ell) - \boldsymbol{\mathcal{M}}(0)^T\boldsymbol{\varphi}(0) = \mathbf{d}_e^T\mathbf{Q}_e^T\boldsymbol{\beta}_e \tag{11}$$

allowing us to directly obtain the discrete form of $\mathcal{W}$ without any FEM interpolation for the kinematic variables $\mathbf{u}(s)$ and $\boldsymbol{\varphi}(s)$. In Eq.(11) the vectors that collect the kinematics $\mathbf{d}_e$ and static $\boldsymbol{\beta}_e$ FE generalized parameters and the compatibility operator $\mathbf{Q}_e$ are defined as

$$\boldsymbol{\beta}_e = \begin{bmatrix} N_1 \\ M_2(0) \\ M_3(0) \\ M_2(\ell) \\ M_3(\ell) \\ M_1 \end{bmatrix}, \quad \mathbf{d}_e = \begin{bmatrix} \mathbf{u}(0) \\ \boldsymbol{\varphi}(0) \\ \mathbf{u}(\ell) \\ \boldsymbol{\varphi}(\ell) \end{bmatrix}, \quad \mathbf{Q}_e = \frac{1}{\ell}\begin{bmatrix} -\ell\,\mathbf{i}_1^T & \mathbf{0} & \ell\,\mathbf{i}_1^T & \mathbf{0} \\ \mathbf{i}_3^T & -\ell\,\mathbf{i}_2^T & -\mathbf{i}_3^T & \mathbf{0} \\ -\mathbf{i}_2^T & -\ell\,\mathbf{i}_3 & \mathbf{i}_2^T & \mathbf{0} \\ -\mathbf{i}_3^T & \mathbf{0} & \mathbf{i}_3^T & \ell\,\mathbf{i}_2^T \\ \mathbf{i}_2^T & \mathbf{0} & -\mathbf{i}_2^T & \ell\,\mathbf{i}_3^T \\ \mathbf{0} & -\ell\,\mathbf{i}_1^T & \mathbf{0} & \ell\,\mathbf{i}_1^T \end{bmatrix}. \tag{12}$$

2.3 Shakedown problem

We say that a structure shakes down to an elastic state or, simply, shakedown occurs if, after an initial phase during which the occurrence and the accumulation of plastic strain increments are possible, the structural response, for every load path, tends to be purely elastic and is characterized by a finite total plastic work.

2.3.1 Load domain

The FE external load vector $\mathbf{p}(t)$, varying with the time t, can be expressed as a combination of p load patterns $\mathbf{p}_i$ belonging to an admissible *load domain* $\mathbb{P}$. We assume

$$\mathbb{P} := \bigcup_{k=1}^{q} \mathbb{P}^{(k)}, \quad \mathbb{P}^{(k)} := \left\{ \mathbf{p} = \sum_{i=1}^{p} \alpha_{ki}(t)\mathbf{p}_i : \alpha_{ki}^{min} \leq \alpha_{ki}(t) \leq \alpha_{ki}^{max} \right\} \tag{13}$$

where α_{ki} defines the range of variability in time of $\mathbf{p}_i$ for the kth load combination accounting for the probability of simultaneous actions. Each combination $\mathbb{P}^{(k)}$ is a convex polytope with 2^p vertexes.

2.3.2 Melan's shakedown theorem and admissibility condition

For frames with medium to large span to depth ratios of the members, it is a reasonable approximation to define the elastic domain only in terms of normal stress components $\sigma \equiv \sigma_{11}$. In this case, it is useful to define the envelope of elastic stress $\mathbb{S}(s, \mathbf{x})$ associated to a generic point of the body $(s, \mathbf{x})$ as the set of elastic stresses $\hat{\sigma}(s, \mathbf{x})$ produced by all loads $\mathbf{p} \in \mathbb{P}$. With these assumptions, the static shakedown theorem can be formulated as follows: shakedown occurs if there exists an additional time-independent self-equilibrated stress $\sigma(s, \mathbf{x})$ such that

$$f_c(s, \mathbf{x}) \leq \lambda \hat{\sigma}(s, \mathbf{x}) + \sigma(s, \mathbf{x}) \leq f_t(s, \mathbf{x}), \qquad \forall \hat{\sigma}(s, \mathbf{x}) \in \mathbb{S}(s, \mathbf{x}) \tag{14}$$

where $f_t(s, \mathbf{x})$ and $f_c(s, \mathbf{x})$ are the stress limits of the material in traction (positive) or compression (negative) respectively. An amplification factor λ of the reference load domain is introduced. This makes it possible to define the shakedown safety factor of the reference load domain as the maximum value of λ for which shakedown occurs.

2.3.3 Shakedown yield function

The shakedown admissibility condition (14) for a load domain amplified by λ, omitting the dependence from s and $\mathbf{x}$, can be written in terms of stress envelope endpoints as

$$\begin{cases} \sigma + \lambda \hat{\sigma}^{\max} \leq f_t \\ \sigma + \lambda \hat{\sigma}^{\min} \geq f_c. \end{cases} \tag{15}$$

This rewriting allows us to introduce the *shakedown yield function* $f(\sigma, \lambda)$

$$f(\sigma, \lambda) \equiv |\sigma - c(\lambda)| - r(\lambda) \leq 0 \tag{16}$$

where

$$\begin{aligned} c = c_0 - \lambda \hat{c} \quad &\text{with} \quad c_0 = \frac{f_t + f_c}{2} \quad \hat{c} = \frac{\hat{\sigma}^{\max} + \hat{\sigma}^{\min}}{2} \\ r = r_0 - \lambda \hat{r} \quad &\text{with} \quad r_0 = \frac{f_t - f_c}{2} \quad \hat{r} = \frac{\hat{\sigma}^{\max} - \hat{\sigma}^{\min}}{2} \end{aligned} \tag{17}$$

Condition in Eq.(16) defines the admissible domain of the additional self-equilibrated stress σ that depends on the load amplifier λ. We can note how this domain is unrelated to the complexity of the load variation, but depends only on the maximum $\hat{\sigma}^{\max}$ and minimum $\hat{\sigma}^{\min}$ elastic effect on the point, apart from the material strength.

It is important to remark the first important feature of the proposed approach: only the two vertexes of the elastic envelope of each fiber affect the admissible domain, independently from the number of basic actions or the complexity of the load domain.

2.3.4 Shakedown safety factor for the fiber model

According to a fiber FE concept, the admissibility condition is imposed at a discrete number of points belonging to the FE domain. To this end, a certain number of integration points (IPs) (cross sections) are used along the beam axis. Gauss-Lobatto rules are preferred in order to include the check at the end sections. At least 3 Gauss-Lobatto IPs are needed to exactly integrate the elastic complementary energy along the element

$$\frac{1}{2}\boldsymbol{\beta}_e^T \mathbf{H}_e \boldsymbol{\beta}_e = \frac{1}{2}\sum_g \mathbf{n}_g^T \mathbf{E}_g^{-1} \mathbf{n}_g w_g + \frac{1}{2}\sum_g \boldsymbol{\tau}_g^T \mathbf{G}_g^{-1} \boldsymbol{\tau}_g w_g \tag{18}$$

but more than 3 points can be used for a more accurate check of the admissibility condition. Note that a generic integration point quantity $(.)_g$ belongs to a FE e but the subscript e is omitted to simplify the notation. For each IP, the cross section is discretized using a finite number n_f of fibers with a normal stress σ constant over each fiber domain of area A and equal to the mid point one. The complementary energy density of the section, on the basis of Eq.(8), can then be evaluated as

$$\frac{1}{2}\mathbf{n}_g^T \mathbf{E}_g^{-1} \mathbf{n}_g = \frac{1}{2}\sum_m \frac{1}{E_m}\sigma_m^2 A_m \tag{19}$$

where E is the Young modulus and the subscript m denotes a generic fiber. Also in this case, a generic fiber quantity $(.)_m$ belongs to an IP g and a FE e, but subscripts g and e are omitted to simplify the notation. Remembering that the fiber strain is linked to the generalized ones as $\epsilon_m = \mathbf{a}_m^T \boldsymbol{\varepsilon}$ and the elastic law $\sigma = E\epsilon$, the previous equation allows us to evaluate $\mathbf{E}_g$ as

$$\sum_m E_m \epsilon_m^2 A_m = \frac{1}{2}\boldsymbol{\varepsilon}_g^T \left(\sum_m E_m \mathbf{a}_m \mathbf{a}_m^T\right) \boldsymbol{\varepsilon}_g \quad \Rightarrow \quad \mathbf{E}_g = \left(\sum_m E_m \mathbf{a}_m \mathbf{a}_m^T\right)$$

For the fiber model, the normal stress resultants in Eq. (4) on the section can be computed as a function of the normal stresses of the fibers at IP, collected in vector $\boldsymbol{\sigma}_g = [\sigma_1, \cdots, \sigma_{nf}]$, as

$$\mathbf{n}_g(\boldsymbol{\sigma}_g) = \sum_m \sigma_m A_m \mathbf{a}_m. \tag{20}$$

We have that the vector collecting all stress resultants can be written, exploiting Eq.(7), as

$$\mathbf{t}_g(\boldsymbol{\sigma}_g, \boldsymbol{\tau}_g) = \begin{bmatrix} \mathbf{n}_g \\ \boldsymbol{\tau}_g \end{bmatrix} \equiv \mathbf{T}_n^T \sum_m (\sigma_m A_m \mathbf{a}_m) + \mathbf{T}_\tau^T \boldsymbol{\tau}_g. \tag{21}$$

The shakedown safety factor λ_S of the discretized structure can be obtained by solving the following constrained optimisation problem

$$\begin{aligned}
\text{maximize} \quad & \lambda \\
\text{subject to} \quad & \mathbf{Q}^T \boldsymbol{\beta} = \mathbf{0} \\
& f(\sigma_m, \lambda) \le 0 && \forall e, g, m \\
& \mathbf{t}_g(\boldsymbol{\sigma}_g, \boldsymbol{\tau}_g) - \mathbf{L}_g \boldsymbol{\beta}_e = \mathbf{0} && \forall g, e
\end{aligned} \tag{22}$$

where the last equality constraint is necessary to preserve the equilibrated stress interpolation (9) over the element. We can note that (22) is very similar to the static limit analysis optimization problem. In particular, the only relevant difference is that the plastic admissibility is imposed for the two vertexes of $\mathbb{S}(s, \mathbf{x})$. Shakedown analysis reduces to limit analysis when the stress envelope degenerates into a single point [6].

3   INCREMENTAL-ITERATIVE SHAKEDOWN ANALYSIS

In this section, we show how to solve the shakedown optimization problem in Eq.(22) by using an incremental-iterative continuation strategy. To this aim, we define a sequence of non-decreasing safe load multipliers converging to the shakedown safety factor.

3.1   Sequence of safe load multiplier converging to the shakedown safety factor

Let us denote with $\mathbf{z} = \{\lambda, \boldsymbol{\beta}, \mathbf{d}, \boldsymbol{\tau}_g, \boldsymbol{\sigma}_g, \boldsymbol{\rho}_g\}$ the set of all the problem variables. It is possible to define a sequence of states $\mathbf{z}^{(n)}$ corresponding to a non-decreasing sequence of load factors $\lambda^{(n)}$ converging to the shakedown limit (Eq.(22)). A superscript (n) denotes the searched solution at the new step of the sequence. $\Delta(.) = (.)^{(n)} - (.)^{(n-1)}$ represents the difference between quantities of step (n) and $(n-1)$. We introduce the following non-negative energy term

$$\Psi_g(\Delta\boldsymbol{\sigma}_g, \Delta\boldsymbol{\tau}_g) = \frac{1}{2} \sum_m \frac{1}{E_m} \Delta\sigma_m^2 A_m w_g + \frac{1}{2} \Delta\boldsymbol{\tau}_g^T \mathbf{G}_g^{-1} \Delta\boldsymbol{\tau}_g w_g \tag{23}$$

which represents a norm of the stress increment. The problem variables at the new step $\mathbf{z}^{(n)}$, omitting the superscript (n) to simplify the notation, that correspond to an assigned $\lambda = \bar{\lambda} \ge \lambda^{(n-1)}$, are obtained as the solution of the following optimization problem

$$\begin{aligned}
\text{minimize} \quad & \sum_{e,g} \Psi_g(\Delta\boldsymbol{\sigma}_g, \Delta\boldsymbol{\tau}_g) \\
\text{subject to} \quad & \mathbf{Q}^T \boldsymbol{\beta} = \mathbf{0} \\
& f_m(\bar{\lambda}, \sigma_m) \le 0 && \forall m, g, e \\
& \mathbf{t}_g(\boldsymbol{\sigma}_g, \boldsymbol{\tau}_g) - \mathbf{L}_g \boldsymbol{\beta}_e = \mathbf{0} && \forall g, e
\end{aligned} \tag{24}$$

i.e. by finding the increment of self-equilibrated stress with minimum norm (23) which makes it possible to fulfill the sufficient condition of the lower bound shakedown theorem for $\bar{\lambda} = \lambda^{(n)}$ to be safe. Clearly, the sequence $\lambda^{(n)}$ can start from $\lambda^{(0)} = \lambda_E$ since no additional stresses are needed for $\lambda < \lambda_E$. It is necessary to note that Eq.(24) admits solution only if $\lambda^{(n)} \leq \lambda_S$ because, by definition, no additional self-equilibrated stress able to satisfy the admissibility condition can be found beyond λ_S. This suggests that it is not convenient to directly assign the values of $\lambda^{(n)}$. Instead, we can use a continuation strategy replacing $\lambda = \bar{\lambda}$ with an arc-length equation for defining $\mathbf{z}^{(n)}$ [7]:

$$g(\Delta \mathbf{d}, \Delta \lambda) - \Delta \xi = 0. \tag{25}$$

At each step, the self-equilibrium of the additional stress and can be collected in the group of global equations together with Eq.(25):

$$\text{Global equations} \quad \begin{cases} \mathbf{Q}^T \boldsymbol{\beta} = \mathbf{0} \\ g(\Delta \mathbf{z}) - \Delta \xi = 0. \end{cases} \tag{26a}$$

Element-wise equations preserve the kinematic compatibility of $\Delta \boldsymbol{\rho}_g$ with $\Delta \mathbf{d}_e$ and the FE equilibrated stress interpolation in Eq.(9):

$$\text{Element equations} \quad \begin{cases} \mathbf{Q}_e \Delta \mathbf{d}_e - \sum_g \mathbf{L}_g^T \Delta \boldsymbol{\rho}_g w_g = \mathbf{0} \\ \mathbf{t}_g(\boldsymbol{\sigma}_g, \boldsymbol{\tau}_g) - \mathbf{L}_g \boldsymbol{\beta}_e = \mathbf{0} \quad \forall g \end{cases} \quad \forall e. \tag{26b}$$

Finally, constitutive laws at each IP link the section stress resultants $\mathbf{t}_g$ to the section generalized strain increment $\Delta \boldsymbol{\rho}_g$:

$$\text{Constitutive equations} \quad \begin{cases} \text{Fiber stress } \sigma \quad \begin{cases} \Delta \sigma_m - E_m \left(\Delta \epsilon_m - \mu_m \dfrac{\partial f_m(\lambda, \sigma_m)}{\partial \sigma_m} \right) = 0 \\ \mu_m \geq 0 \quad \mu_m f_m(\lambda, \sigma_m) = 0 \end{cases} \\ \text{Tangential stress resultants} \quad \Delta \boldsymbol{\tau}_g = \mathbf{G}_g \mathbf{T}_\tau \Delta \boldsymbol{\rho}_g \end{cases} \tag{26c}$$

where $\Delta \epsilon_m = \mathbf{a}_m^T \Delta \boldsymbol{\varepsilon}$, with $\Delta \boldsymbol{\varepsilon} = \mathbf{T}_n \Delta \boldsymbol{\rho}_g = [\Delta e, \Delta \chi_2, \Delta \chi_3]^T$, denotes the increment of strain work-conjugate to σ_m

$$\Delta \epsilon_m = \Delta e + \Delta \chi_2 x_{3m} - \Delta \chi_3 x_{2m}.$$

The first of Eqs.(26c), for an assigned $\Delta \boldsymbol{\rho}_g$ and then $\Delta \epsilon_m$, is the elasto-plastic constitutive law of the fiber m integrated by a backward Euler scheme and can be seen as the first order condition of the following CPP problem:

$$\begin{cases} \text{minimize} \quad \dfrac{1}{2} E_m (\sigma_m - \sigma_m^*)^2 \\ \text{subject to} \quad f_m(\lambda, \sigma_m) \leq 0 \end{cases} \quad \forall m \tag{27}$$

with the fiber elastic predictor $\sigma_m^* = \sigma_m^{(n-1)} + E_m \Delta \varepsilon_m$. The solution of this one-dimensional optimization problem is straightforward and just requires a min-max scalar operation:

$$\sigma_m = \max \left(f_c - \lambda \hat{\sigma}_{min}, \; \min \left(\sigma_m^*, \; f_t - \lambda \hat{\sigma}_{max} \right) \right). \tag{28}$$

Equations (26) define the *elasto-plastic* shakedown step since are very similar to the step equations of a standard incremental elasto-plastic analysis. The main difference is that the admissible domain for the self-equilibrated stress σ is a function of the load factor λ. The fiber based approach makes it possible to avoid complex multisurface optimization problems on the section required when the elastic domain is expressed in terms of stress resultants (see [4]), along with a straightforward definition of the elastic stress envelope for multiple load combinations. The proof of convergence of the load factor sequence to the shakedown safety factor is given in [5]. The main advantage of the proposed incremental process is that it does not require any constrained optimization algorithm.

3.2 Decomposed strain-driven solution algorithm

The formulation presented in the previous section allows us to evaluate the shakedown safety factor by means of a sequence of increments. At each increment the current estimate of the load factor can be obtained by solving Eq.s (26). Such equations are subdivided into three groups: global equations, element equations and constitutive equations. Instead of solving Eqs.(26) all together, it is possible to apply a strain-driven decomposed strategy based on the solution of the following three nested sub-steps.

- A *section state determination* provides the stress resultants $\mathbf{t}_g$ at each IP along the beam axis as a function of an assigned section generalized strain increment $\Delta \boldsymbol{\rho}_g$ and the current estimate of the load factor λ by means of the constitutive law (26c).

- An *element state determination* finds the element stress interpolation variables $\boldsymbol{\beta}_e$ corresponding to an assigned increment of element nodal kinematic variables $\Delta \mathbf{d}_e$ and the current load factor estimate λ by means of the element equations (26b). This require an element-wise iterative solution involving, at each iteration, a section state determination at the IPs.

- A *global analysis* uses an iterative process to find the solution of the global equations (26a) with the stress interpolation variables $\boldsymbol{\beta}$ written as functions of the unknown global kinematic degrees of freedom $\mathbf{d}$ and the current load factor λ through the element state determination.

Section state determination, element state determination and global solution are described in details in [5]. The same algorithm was used in [8] to evaluate the time of fire exposure leading to collapse.

4 NUMERICAL TESTS AND CONCLUSIONS

In this section, a numerical application is illustrated. The computational cost of the analyses can be assessed in terms of total number of global iterations, each of them
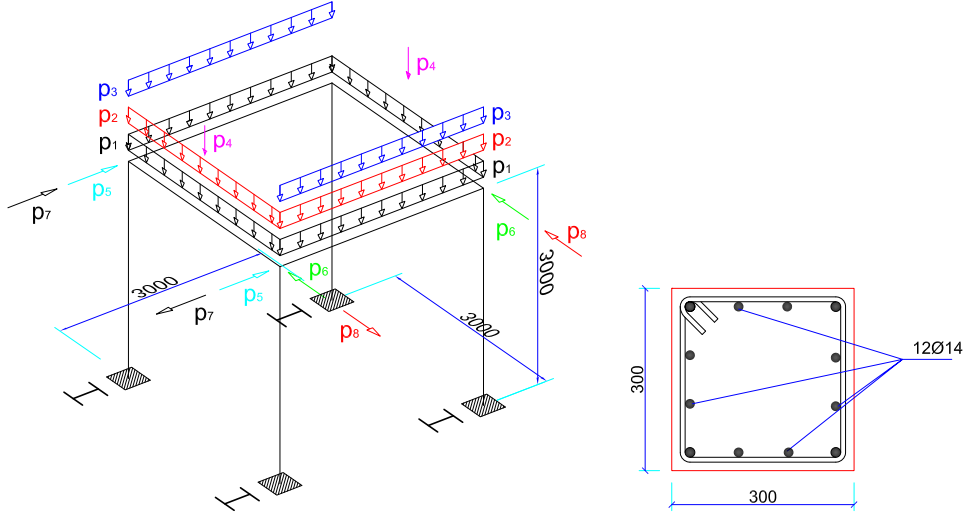
Figure 2: Loads and geometry for the simple 3D frame.

dominated by the decomposition of the tangent stiffness matrix. Three material types are used for the cross sections: i) structural steel with $E = 210000MPa$, $f_c = -300MPa$ and $f_t = 300MPa$; ii) concrete with $E = 25000MPa$, $f_c = -30MPa$ and $f_t = 0$; iii) reinforcing steel bars with $E = 210000MPa$, $f_c = -400MPa$ and $f_t = 400MPa$. The test regards the simple 3D frame under variable actions shown in Fig.2. The polyhedral load domain, adopting a single load combination, is defined as follows

$$\mathbf{p}(t) = \sum_{k=1}^{8} \alpha_k \mathbf{p}_k \quad \begin{cases} 1.1 \leq \alpha_1(t) \leq 1.3 \\ 0.0 \leq \alpha_k(t), \leq 1.5, \quad k = 2 \cdots 4 \\ -1.0 \leq \alpha_k(t), \leq 1.0, \quad k = 5 \cdots 8 \end{cases}$$

The magnitudes of the distributed and concentrated loads are $p_1 = 22.5kN/m$, $p_2 = 30kN/m$, $p_3 = 15kN/m$, $p_4 = 45kN$, $p_5 = \cdots = p_8 = 4.5kN$. Two material configurations are considered. In the first one, all members have the RC section reported in Fig.2. A steel HEA240 section is used for all members in the second one. These simple configurations are selected in order to make this test easily reproducible. Two FEs are employed for each beam, while a single element per column is used. A mesh refinement does not provide any difference because of the equilibrated stress interpolation. Flanges and web of HE section are discretized using $n_l \times n_t$ fibers, n_t through the thickness and n_l along the orthogonal direction. A uniform $n_f \times n_f$ discretization is used for the concrete part of RC sections, while reinforcing bars are modeled using a single fiber per bar with area concentrated at the bar center. The RC section is supposed to be confined in such a way that concrete has a sufficient ductility in compression. 3 Gauss-Lobatto IPs per FE are used since no difference in the shakedown safety factor has been observed with 5 and 7 points. Figure 3 shows the pseudo-equilibrium path for the 2 material configurations varying the number of fibers. It is possible to observe how the incremental-iterative process quickly converges at the shakedown safety factor. 10×10 fibers give accurate results for the RC section,
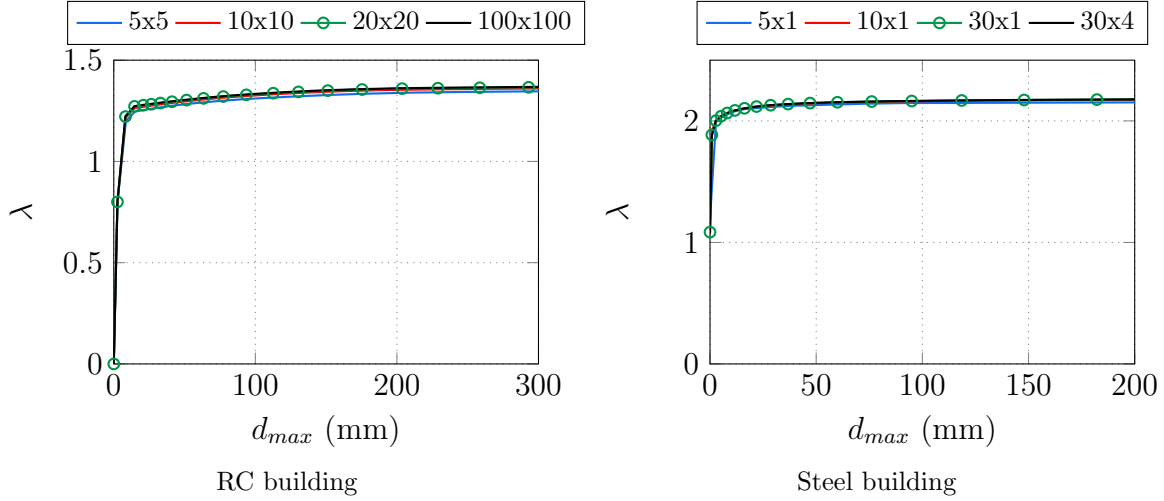
Figure 3: Pseudo-equilibrium path varying the number of fibers.

according to Tab.1, while 10×1 fibers per wall give practically the exact solution for the steel section, as reported in Tab.2. In the same tables, the number of steps, the total number of global iterations and the average number of FE iterations for each element state determination is also reported. Around 15-20 steps provide a converged safety factor for both RC and steel material. The number of total global iterations is generally quite small, higher in the RC case compared to the steel one, while each element state determination converges with an average number of 2-3 iterations. The computational cost is then very similar to that of a standard incremental elasto-plastic analysis. Finally, the number of fibers does not affect significantly neither the global nor the element iterative burden.

fibers	λ_S	steps	total global iters	mean FE iters
5×5	1.35	19	72	2.64
10×10	1.36	18	64	2.57
20×20	1.37	20	94	2.70
100×100	1.37	19	75	2.92

Table 1: RC frame: shakedown safety factor, number of steps, total number of global iterations and average number of iterations for the element state determination

fibers	λ_E	λ_S	steps	total global iters	mean FE iters
5×1	1.19	2.15	15	37	1.93
10×1	1.13	2.17	16	40	1.88
30×1	1.08	2.18	17	42	1.95
30×4	1.07	2.18	18	49	2.03

Table 2: Steel frame: shakedown safety factor, number of steps, total number of global iterations and average number of iterations for the element state determination.

REFERENCES

[1] R. Casciaro, G. Garcea, An iterative method for shakedown analysis, Computer Methods in Applied Mechanics and Engineering 191 (49-50) (2002) 5761–5792.

[2] D. Magisano, F. Liguori, L. Leonetti, G. Garcea, Minkowski plasticity in 3D frames: Decoupled construction of the cross-section yield surface and efficient stress update strategy, International Journal for Numerical Methods in Engineering 116 (7) (2018) 435–464. doi:10.1002/nme.5931.

[3] D. Magisano, F. Liguori, L. Leonetti, D. de Gregorio, G. Zuccaro, G. Garcea, A quasi-static nonlinear analysis for assessing the fire resistance of reinforced concrete 3D frames exploiting time-dependent yield surfaces, Computers & Structures 212 (2019) 327 – 342. doi:https://doi.org/10.1016/j.compstruc.2018.11.005.

[4] L. Leonetti, R. Casciaro, G. Garcea, Effective treatment of complex statical and dynamical load combinations within shakedown analysis of 3D frames, Computers & Structures 158 (2015) 124 – 139. doi:https://doi.org/10.1016/j.compstruc.2015.06.002.

[5] D. Magisano, G. Garcea, Fiber-based shakedown analysis of three-dimensional frames under multiple load combinations: Mixed finite elements and incremental-iterative solution, International Journal for Numerical Methods in Engineering 121 (17) (2020) 3743–3767. doi:https://doi.org/10.1002/nme.6380.

[6] G. Garcea, L. Leonetti, A unified mathematical programming formulation of strain driven and interior point algorithms for shakedown and limit analysis, International Journal for Numerical Methods in Engineering 88 (11) (2011) 1085–1111. doi:10.1002/nme.3188.

[7] D. Magisano, L. Leonetti, G. Garcea, How to improve efficiency and robustness of the Newton method in geometrically non-linear structural problem discretized via displacement-based finite elements, Computer Methods in Applied Mechanics and Engineering 313 (2017) 986–1005. doi:10.1016/j.cma.2016.10.023.

[8] D. Magisano, G. Garcea, Limit fire analysis of 3D frame structures, Engineering Structures 233 (2021) 111762. doi:https://doi.org/10.1016/j.engstruct.2020.111762.